magnetochemistry

MDPI

Article

Magnetostructural Studies on Zigzag One-Dimensional Coordination Polymers Formed by Tetraamidatodiruthenium(II,III) Paddlewheel Units Bridged by SCN Ligands

Sara Moreno-Da Silva [1], Patricia Delgado-Martínez [2], Miguel Cortijo [1], Rodrigo González-Prieto [1], José Luis Priego [1,*], Santiago Herrero [1] and Reyes Jiménez-Aparicio [1,*]

[1] Departamento de Química Inorgánica, Facultad de Ciencias Químicas, Universidad Complutense de Madrid, Ciudad Universitaria, E-28040 Madrid, Spain
[2] Centro de Asistencia a la Investigación Difracción de Rayos X, Facultad de Ciencias Químicas, Universidad Complutense de Madrid, E-28040 Madrid, Spain
* Correspondence: bermejo@ucm.es (J.L.P.); reyesja@ucm.es (R.J.-A.)

Received: 27 May 2019; Accepted: 12 June 2019; Published: 1 July 2019

Abstract: We report herein on three zigzag one-dimensional coordination polymers of {[Ru_2(μ-NHOCR)$_4$](μ-SCN)}$_n$ (R = *o*-Me-C_6H_4 (**2**), *m*-Me-C_6H_4 (**3**), *p*-Me-C_6H_4 (**4**)) formula. These new compounds have been obtained by reaction of the corresponding [Ru_2(μ-NHOR)$_4$(THF)$_2$](BF_4) complex with (NBu_4)(SCN) under different synthetic conditions. The crystal structure of [Ru_2(μ-NHOC$_6H_4$-*o*-Me)$_4$(THF)$_2$](BF_4) (**1**), **2** and **3** are presented. A *cis*-(2,2) arrangement of the amidate ligands of the [Ru_2(μ-NHOCR)$_4$]$^+$ units is observed in all cases. Interestingly, the structures of **2** and **3** show linkage isomerism in alternated tetraamidatodiruthenium units whose axial positions are occupied by the same type of donor atom of the SCN ligands. This results in zigzag chains with a Ru-S-C angle of 98.97° and Ru-N-C angle of 169.36° in the case of **2** and 97.99° and 159.26°, respectively, in the case of **3**. The magnetic data obtained for **2**–**4** are indicative of a $\sigma^2\pi^4\delta^2(\pi^*\delta^*)^3$ ground state (S = 3/2) and a large zero-field splitting (ZFS) in all cases (D = 54.57, 62.72 and 43.00 cm^{-1} for **2**–**4**, respectively). Similar small antiferromagnetic interactions between diruthenium units (zJ = −0.93, −0.79 and −1.11 cm^{-1} for **2**–**4**, respectively) are estimated for all the polymers, suggesting an analogous zigzag arrangement of the chains for **4**.

Keywords: diruthenium; 1-D zigzag compounds; coordination polymers; antiferromagnetic interactions; amidate complexes; thiocyanate compounds

1. Introduction

Tetraamidato compounds [Ru_2X(μ-NHOCR)$_4$] (X = halide ion) are types of Ru_2^{5+} paddlewheel complexes with four N,O-donor ligands bridging the two ruthenium atoms [1–5]. The paramagnetic [Ru_2(μ-NHOCR)$_4$]$^+$ units (S = 3/2) are linked by halide ions giving zigzag chains and the unpaired electrons are essentially delocalized over the Ru-Ru bond, making the compounds formally valent-averaged compounds. In these polymeric complexes four different isomers are possible depending on the bridging coordination mode of the amidate ligands (Figure 1).

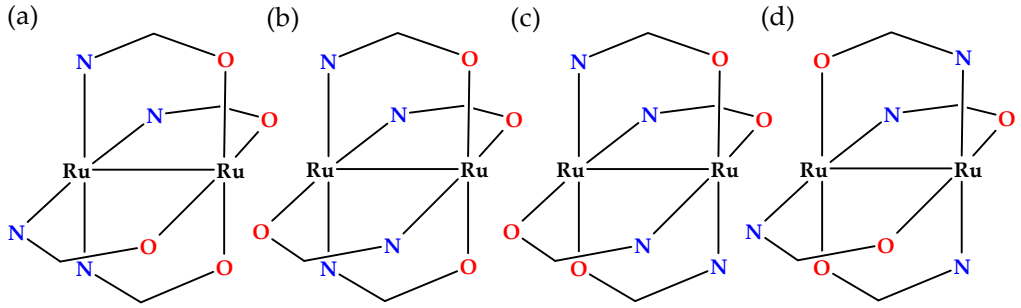

Figure 1. Schematic representation of the possible isomers of the $[Ru_2(\mu\text{-}NHOCR)_4]^+$ compounds: (**a**) 4,0-; (**b**) 3,1-; (**c**) *cis*-(2,2); (**d**) *trans*-(2,2).

Although the amidato compounds have been less studied than the tetracarboxylato analogues—$[Ru_2X(\mu\text{-}O_2CMe)_4]$—an important number of amidato compounds has been described. In contrast to the carboxylato compounds, which are usually obtained by metathesis reaction from $[Ru_2Cl(\mu\text{-}O_2CMe)_4]$ with the corresponding carboxylate ligand, the amidato compounds must be obtained in more drastic reaction conditions because the substitution of the acetate ligand in $[Ru_2Cl(\mu\text{-}O_2CMe)_4]$ by amides is not favoured [6–11]. This drawback has limited the study of tetraamidato compounds and also their insolubility makes the preparation of single crystals difficult. Therefore, the number of crystal structures described in the literature is scarce [9,10,12–15]. Recently, new non-conventional experimental methods such as solvothermal or microwave activation have been successfully used to prepare single crystals of amidato compounds [12–14]. In general, the majority of the tetraamidatodiruthenium compounds described in the literature form infinite zigzag chains with the diruthenium units bonded by halide ligands [9,10,12–15]. Non-halide linkers are unknown in tetraamidatodiruthenium compounds, with the exception of $[\{Ru_2(acam)_4\}_2(M'O_4)]$ (M' = Cr, Mo, W; Hacam = acetamide) [16]. Moreover, it must be pointed out that although there are four possible isomers for the $[Ru_2(\mu\text{-}NHOCR)_4]^+$ compounds (Figure 1a–d), there is not any reported example showing the a or the b structure.

On the other hand, the thiocyanate ion is a very useful ligand for the synthesis of homo- and hetero-bimetallic coordination polymers due to their duality in the softness/hardness coordination sites and the inherent coordination angle that varies between 4 and 60°. In general, the thiocyanate ion is bounded through the N atom to first-row transition metals whereas it is coordinated through the S atom to heavier transition metal ions. However, other factors such as oxidation state of the metal, steric hindrance, electronic structure of the ancillary ligands or the nature of the solvent have also influence in the final coordination mode of the thiocyanate ligand [17]. In some cases, both N- and S-bonded isomers have been isolated and crystallographically characterized [18–22]. In some complexes, several coordination modes coexist, for example in $[Fe(tpc\text{-}OBn)(NCS)(\mu\text{-}NCS)_2]$ (tpc-OBn = *tris*(2-pyridyl)benzyloxymethane), which has μ-κN:κS-SCN and terminal κN-SCN thiocyanate ligands [21]. Linear chain polymers containing metal ions joined by pairs of thiocyanate ligands with *trans*-N and *trans*-S coordination are usually found [22,23]. However, the formation of chains in which only one thiocyanate ligand acts as bridge is less frequent [24].

Although the interaction between tetraamidatodiruthenium compounds and SCN ligands are unknown, some examples of other diruthenium complexes with SCN have been described. To our knowledge, only four crystal structures have been published: Ionic zigzag chains in the $[C(NH_2)_3]_4[Ru_2(hedp)_2(SCN)]\cdot 4H_2O$ (hedp = 1-hydroxyethylidenediphosphonate) complex [25] and three molecular species, $[Ru_2(O_2CMe)(DPhF)_3(NCS)]$ (DPhF = *N*,*N*′-diphenylformamidinate) [26], $[Ru_2(F_3ap)_4(NCS)]$ and $[Ru_2(F_3ap)_3(F_2Oap)(NCS)]$ (F_3ap = 2-(2,4,6-trifluoroanilino)pyridinate anion) [27].

In this work we have used several tetraamidatodiruthenium units and thiocyanate ligands in order to prepare zigzag one-dimensional compounds, to determine their crystal structure and to study their magnetic properties. Thus, the reaction of $[Ru_2(\mu\text{-}NHOR)_4(THF)_2](BF_4)$ with $(NBu_4)(SCN)$ leads to zigzag one-dimensional coordination polymers with $[\{Ru_2(\mu\text{-}NHOCR)_4\}(\mu\text{-}SCN)]_n$ (R = *o*-Me-C_6H_4

(**2**), *m*-Me-C_6H_4 (**3**), *p*-Me-C_6H_4 (**4**)) formula. These new compounds have been obtained by reaction of the corresponding starting materials under different synthetic conditions. The crystal structure of the intermediate $[Ru_2(\mu\text{-}NHOCC_6H_4\text{-}o\text{-}Me)_4(THF)_2](BF_4)$ (**1**) has also been obtained.

2. Results and Discussion

2.1. Synthesis and Spectroscopic Characterization

The $[Ru_2Cl(\mu\text{-}NHOCR)_4]_n$ compounds (R = *o*-Me-C_6H_4, *m*-Me-C_6H_4, *p*-Me-C_6H_4) were used as starting materials. The reaction of these compounds with $AgBF_4$ in THF gives the intermediate compounds, $[Ru_2(\mu\text{-}NHOCR)_4(THF)_2](BF_4)$, that were used in a subsequent reaction without isolation. $[Ru_2(\mu\text{-}NHOCC_6H_4\text{-}o\text{-}Me)_4(THF)_2](BF_4)$ (**1**) was crystallographically characterized in order to confirm the nature of these species. The reaction of the intermediate complexes with a high excess of $(NBu_4)(SCN)$ in methanol yielded the 1D zigzag coordination polymers, $[Ru_2(SCN)(\mu\text{-}NHOCR)_4]_n$ (R = *o*-Me-C_6H_4 (**2**), *m*-Me-C_6H_4 (**3**), *p*-Me-C_6H_4 (**4**).

$$[Ru_2Cl(\mu - NHOCR)_4]_n + AgBF_4 \overset{THF}{\rightarrow} [Ru_2(\mu - NHOCR)_4(THF)_2](BF_4) + AgCl$$

$$[Ru_2(\mu - NHOCR)_4(THF)_2](BF_4) + (NBu_4)(SCN) \overset{MeOH}{\rightarrow} [Ru_2(\mu - NHOCR)_4(SCN)]_n + (NBu_4)(BF_4)$$

$$(R = Me - o - C_6H_4,\ Me - m - C_6H_4,\ Me - p - C_6H_4)$$

The reactions of the $[Ru_2(\mu\text{-}NHOCR)_4(THF)_2](BF_4)$ compounds with $(NBu_4)(SCN)$ were carried out by conventional, solvothermal and microwave-assisted solvothermal methods. More details about the reaction conditions are shown in Table 1 and in the Materials and Methods section. The best yields were obtained in the syntheses of **4** and the lowest yields in the preparation of **2**. This is probably caused by the different steric hindrance of the *ortho*, *meta* and *para* configurations. All the attempts made to obtain **2**–**4** by direct reaction of $[Ru_2Cl(\mu\text{-}NHOCR)_4]_n$ compounds with AgSCN were unsuccessful. Single crystals of **2** were obtained directly from the solvothermal reaction. The same synthetic conditions did not lead to the formation of single crystals of **3** and **4**. Nevertheless, crystals of **3** were obtained by slow diffusion of a methanol solution of $(NBu_4)(SCN)$ into a THF solution of $[Ru_2(\mu\text{-}NHOCC_6H_4\text{-}m\text{-}Me)_4(THF)_2](BF_4)$.

Table 1. Reaction conditions used to prepare **2**–**4**.

Compound	Method	*T*/°C	$t_{reaction}$ + $t_{cooling}$	Yield/%
2	Conventional	r.t.	48 h + 0	24
	Solvothermal	80	24 h + 16 h	22
	Microwave	80	16 h + 20 min	33
3	Conventional	r.t.	48 h + 0	44
	Solvothermal	80	24 h + 16 h	54
	Microwave	80	16 h + 20 min	33
4	Conventional	r.t.	48 h + 0	66
	Solvothermal	80	24 h + 16 h	63
	Microwave	80	16 h + 20 min	78

The electrospray ionization mass spectra of **2**–**4** do not show the molecular peaks. The base peak corresponds in all cases to the $[Ru_2(\mu\text{-}NHOCCR)_4]^+$ fragment obtained by rupture of the Ru-SCN/NCS bond. The IR spectra of the compounds show the characteristic bands corresponding to the amidate ligands including the ν(N-H) stretching bands in the 3336–3372 cm^{-1} range. Very intense antisymmetric and symmetric stretching CON bands (Amide I and Amide II [14]) due to the bridging equatorial amidate ligands appears in the 1430–1510 cm^{-1} range. Note that these bands can be very close in energy or even give only a broad band. Bands corresponding to the aromatic and aliphatic C-H stretching

modes are also present in all the spectra above and below 3000 cm^{-1}, respectively. Moreover, the IR spectrum of **1** shows a band corresponding to the B-F stretching mode of the BF_4^- anion at 1037 cm^{-1} and the spectra of **2**–**4** show bands corresponding to the C-N stretching mode of the SCN- and NCS-group that are split in the 2014–2077 and 1981–1937 cm^{-1} ranges.

The diffuse reflectance electronic spectra of **2**–**4** in the solid state were also measured (see Table 2). The spectra of these compounds show five bands at similar wavelengths in all cases. The bands observed at 314–269 nm are ascribed to ligand to metal charge transference (LMCT) σ(axial ligand)→σ*(Ru_2) [28–30]. The absorptions observed at *ca*. 360 nm correspond to a LMCT π(O/N)→π*(Ru_2) transition in agreement with the TDDFT-PCM (Time-dependent Density Functional Theory-Polarizable Continuum Method) calculations, described by Cukiernik et al. for tetracarboxylato complexes [31]. The bands at 475–466 nm are caused by π(RuO/N,Ru_2)→π*(Ru_2) transition [32–34], although there may be some additional σ→σ* contribution. The shoulders observed at *ca*. 595 nm are ascribed to σ(Ru-axial ligand)→π*(Ru_2) transitions and the bands in the NIR region at 967–1000 nm are caused by a δ(Ru_2)→δ*(Ru_2) transition [28–30,32].

Table 2. Assignment of the transitions (nm) found in the electronic spectra of **2**–**4**.

Compound	σ(L_{axial}) → σ*(Ru_2)	π(O/N) → π*(Ru_2)	π(RuO/N,Ru_2) → π*(Ru_2)	σ(Ru-L_{axial}) → π*(Ru_2)	δ(Ru_2) → δ*(Ru_2)
2	269	352	466	598sh	967
3	314	360sh	476	592sh	1000
4	299	362sh	475	592sh	989

2.2. Crystal Structures

Single crystal X-ray diffraction measurements were carried out on crystals of **1**–**3**. The structure of these compounds, which crystallize in the*Pī1* space group, is formed by paddlewheel units in which two metal-metal bonded ruthenium atoms are bridged by four amidate ligands. The Ru-Ru distances are 2.2794(8) Å for **1**, 2.3099(18) Å and 2.2954(18) Å for **2** and 2.3131(15) Å and 2.2956(15) Å for **3**. These distances are similar to those found for other tetraamidatodiruthenium(II,III) complexes [8–10,12–15,35,36] and are slightly larger than those found for tetracarboxylatodiruthenium(II,III) complexes [1–5,12,14] because of the higher donor character of the amidate ligands. More bond distances, angles and other crystallographic data are shown in the Supplementary Material (Tables S1–S9). The structure of the three complexes displays an inversion centre in the middle point of the Ru-Ru axis, which leads to a *cis*-(2,2) arrangement of the amidate ligands in the $[Ru_2(\mu\text{-NHOCR})_4]^+$ units. Moreover, in the three structures, the O-Ru-Ru-N torsion angles are very small and almost eclipsed arrangements for the paddlewheel units are observed. Figures S1–S3 show the asymmetric unit of compounds **1**–**3**. All known structures of tetraamidatodiruthenium complexes show a *cis*-(2,2) arrangement of the amidate ligands [8–10,12–15,35–39] with the exception of $[Ru_2Cl(\mu\text{-NHOCC}_6H_4\text{-}o\text{-Me})_4]_n$ [12] and $[Ru_2Br(\mu\text{-NHOCC}_6H_4\text{-}o\text{-Me})_4]_n$ [13] that show a *trans*-(2,2) disposition. The crystal structure of complexes **1**–**3** shows zigzag chains, which is in agreement with a *cis*-(2,2) disposition, as observed in all the other examples of tetraamidato complexes with a zigzag structure. Therefore, the substitution of the chloride in the linear polymer with a *trans*-(2,2) disposition, $[Ru_2Cl(\mu\text{-NHOCC}_6H_4\text{-}o\text{-Me})_4]_n$, by SCN seems to be associated with an isomerization process.

A BF_4^- counterion is present in the structure of **1** that has two THF molecules placed in the axial positions of the diruthenium units (Figure 2, left) similarly to $[Ru_2(\mu\text{-HNOCC}_6H_4\text{-}p\text{-CMe}_3)_4(OPPh_3)_2](BF_4)$ [8] and in several $[Ru_2(\mu\text{-O}_2CR)_4L_2](BF_4)$ compounds [2–4]. Unlike this, the complex $[Ru_2(\mu\text{-NHOCPh})_4(BF_4)(H_2O)]\cdot$2acetone, in which the BF_4^- moiety is unusually coordinated to the axial positions of the dimetallic unit, has been recently reported [39].

π-π stacking is observed between the aromatic rings of neighbour diruthenium units whose centroids are separated by 3.957 Å (See Figure S4). SCN^- ligands bridge the diruthenium units that form the structure of **2** and **3** giving rise to zigzag chains. Two types of alternated diruthenium

units form the structure of **2** and **3**. Each unit has two SCN^- ligands coordinated by the same donor atom—S or N—to the axial positions of it (Figure 2, right). The Ru-S-C and Ru-N-C angles are 98.97° and 169.36° in the structure of **2** and 97.99° and 159.26° in the structure of **3**. The chains are packed mainly by van der Waals forces in both cases. A similar arrangement of the SCN^- ligands with Ru-S-C and Ru-N-C angles (94.7(2)° and 150.2(4)°, respectively) has been found in the analogous complex $[C(NH_2)_3]_4[Ru_2(hedp)_2(SCN)]\cdot 4H_2O$ [25]. The Ru-NCS and Ru-SCN distances are 2.237 Å and 2.621 for **2** and 2.251 Å and 2.643 Å for **3**. These distances are similar to those found in $[C(NH_2)_3]_4[Ru_2(hedp)_2(SCN)]\cdot 4H_2O$. However, the Ru-N distances are larger than the observed in discrete diruthenium complexes with terminal N-bonded SCN^- groups such as $[Ru_2(O_2CMe)(DPhF)_3(NCS)]$ (2.103 Å) [26], $[Ru_2(F_3ap)_4(NCS)]$ (2.123 Å) and $[Ru_2(F_3ap)_3(F_2Oap)(NCS)]$ (2.231 Å) [27] and *trans*-(μ-O,L)-$[Ru_2(\mu\text{-}O)(\mu\text{-}CH_3COO)_2(bpy)_2(L)_2]$ (L = SCN) [2.084(4) Å] [40]. Thus, all known diruthenium compounds with terminal thiocyanate ligands are N-bonded whereas the only polymeric derivative with paddlewheel structure $[C(NH_2)_3]_4[Ru_2(hedp)_2(SCN)]\cdot 4H_2O$ [25] shows the disposition of the SCN^- ligands observed in complex **2** and **3**.

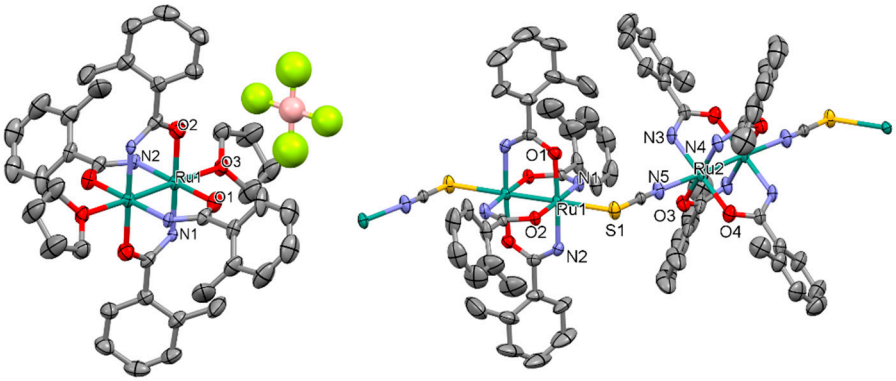

Figure 2. Representations of the structure of **1** (left) and **2** (right) (30% probability ellipsoids). Ruthenium: turquoise; oxygen: red; nitrogen: blue; carbon: grey; boron: pink; fluorine: pale yellow; sulphur: dark yellow. Hydrogen atoms are omitted for clarity.

2.3. Magnetic Properties

The values for the magnetic moments at room temperature ($\mu_{eff.}$) for compounds **2**–**4** are 3.97, 4.37 and 3.90 μ_B, respectively. These values are similar to those found for similar tetraamidatodiruthenium compounds [12–14] and are in accordance with the presence of three unpaired electrons per dimer unit, predicted by the ground-state configuration $\sigma^2\pi^4\delta^2(\pi^*\delta^*)^3$, proposed by Norman et al. [41]. The susceptibility curve for the three compounds shows a continuous increase with decreasing temperature (Figure 3, Figures S5 and S6) typical for paramagnetic compounds. The magnetic moment curve remains almost constant, for compounds **2** and **4** or slightly decreases, for compound **3**, with decreasing temperature until around 100 K, when that decrease becomes more abrupt. This magnetic behaviour has been found in similar polymeric tetraamidato or tetracarboxylatodiruthenium complexes with zigzag chain structure [2–4,12,13,32,42,43] and can be explained by the presence of a large zero-field splitting parameter (D) and weak antiferromagnetic interactions (zJ) between the dimetallic units. The fitting of the magnetic data has been carried out using the model developed by Cukiernik et al. [44], which considers D and the existence of a temperature independent paramagnetism (TIP) and a paramagnetic impurity (P) with $S = 1/2$ due to the possible presence of a ruthenium(III) monomer. A weak antiferromagnetic coupling (zJ) has been considered by using the molecular field approximation [45]. The equation used in this model to fit the molar paramagnetic susceptibility and magnetic moment of these 3/2 spin systems is the following:

$$\chi'_{total} = [(1 - P)\,\chi'] + [P\,Ng_{mo}{}^2\,\beta^2/4kT] \quad (1)$$

where all the parameters mentioned above are included, since

$$\chi'_{total} = [(1 - P)\,\chi'] + [P\,Ng_{mo}{}^2\,\beta^2/4kT]$$

where

$$\chi'_M = \chi_M + TIP$$

and

$$\chi_M = (\chi_{\parallel} + 2\chi_{\perp})/3$$

$$\chi_{\parallel} = (Ng^2\beta^2/kT)\,(1 + 9e^{-2D/kT})/4(1 + e^{-2D/kT})$$

$$\chi_{\perp} = (Ng^2\beta^2/kT)\,[4 + (3kT/D)(1 - e^{-2D/kT})]/4(1 + e^{-2D/kT})$$

In these equations, parameters N, g, zJ, β and k have their typical meanings.

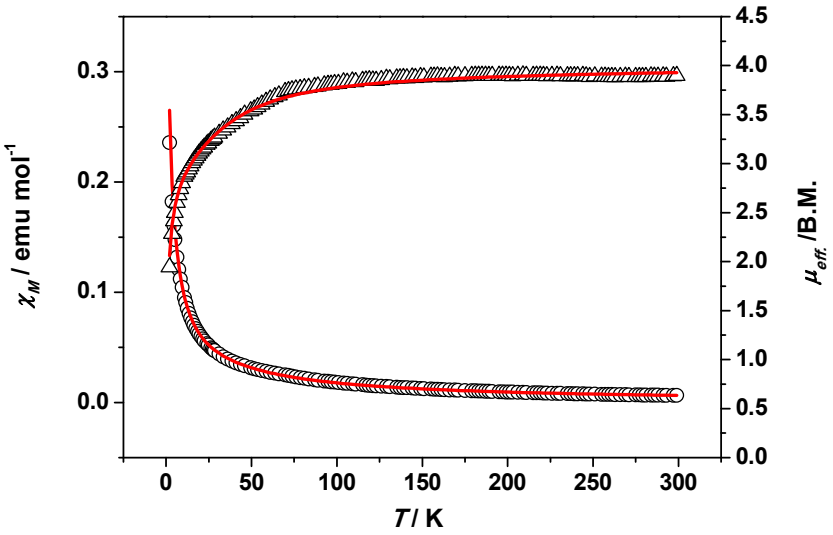

Figure 3. Magnetic molar susceptibility (circles) and magnetic moment (triangles) vs. temperature for compound **4**. Solid lines represent the best fit obtained using the model explained in the text.

Table 3. Magnetic parameters obtained from the fit of the experimental magnetic data of **2**–**4**.

Compound	$\mu_{eff.}$ (R.T., μ_B)	g	D (cm^{-1})	zJ (cm^{-1})	TIP (emu/mol)	P(%)	σ^2
2	3.97	2.05	54.57	−0.93	3.71×10^{-4}	6.29×10^{-5}	3.84×10^{-4}
3	4.37	2.16	62.72	−0.79	8.51×10^{-4}	5.06×10^{-5}	1.58×10^{-5}
4	3.90	2.02	43.00	−1.11	1.48×10^{-4}	2.97×10^{-5}	7.88×10^{-5}

$\sigma^2 = \Sigma(\mu_{eff.\,calcd.} - \mu_{eff.\,exp.})^2/\Sigma\mu_{eff.\,exp.}{}^2$

The use of this model yielded good agreements between the experimental data of the molar paramagnetic susceptibility and magnetic moment with their corresponding calculated data. Figure 3, Figures S5 and S6 show the experimental and calculated curves of magnetic molar susceptibility and magnetic moment versus temperature for compounds **2**–**4**. Table 3 collects the magnetic parameters ($\mu_{eff.}$, D, g, zJ, TIP and P) obtained from the fitting of the experimental values together with the quality of the fits. The obtained values for the zero field splitting parameter are in the range 43.00–62.72 cm^{-1} which are similar for other similar tetraamidato complexes [12–14]. The low negative values obtained for zJ in the three complexes (−0.93, −0.79 and −1.11 cm^{-1}) indicate weak antiferromagnetic interactions between the dimetallic units. These low values are consistent with the zigzag chain structure observed in these complexes, where the magnetic coupling should be propagated through the thiocyanate bridges, although a through-space interaction cannot be ruled out.

3. Materials and Methods

3.1. Materials and Physical Measurements

The $[Ru_2Cl(\mu{-}NHOCR)_4]_n$ (R = *o*-Me-C_6H_4, *m*-Me-C_6H_4 and *p*-Me-C_6H_4) that were employed as starting materials were prepared following a published procedure [12]. The rest of the reactants and solvents were obtained from commercial sources and were used as received. A Memmert Universal Oven UFE 400 and 25 mL Teflon-lined stainless autoclave reactors were employed for the solvothermal syntheses. An ETHOS ONE instrument with temperature and pressure control and 85 mL TFM Teflon-closed vessels were used for the microwave-assisted solvothermal reactions.

The elemental analyses were performed by the Elemental Analysis Service of the Universidad Complutense de Madrid. The FTIR spectra were recorded in the 4000–650 cm^{-1} range using a Perkin–Elmer Spectrum 100 Spectrometer equipped with a universal ATR sampling accessory. Electronic spectra in the solid state were acquired using a Cary 5G spectrophotometer equipped with a Praying Mantis accessory for diffuse reflectance measurements. Mass spectra were obtained by the Mass Spectrometry Service of the Universidad Complutense de Madrid. Electrospray ionization (ESI^+) technique was employed and an ion trap-Bruker Esquire-LC spectrometer was used for the measurements. The magnetic susceptibility data were obtained in the 2–300 K temperature range under a field of 1 T using a Quantum Design MPMSXL Superconducting Quantum Interference Device (SQUID) magnetometer. The samples of **2–4** that were measured were prepared by solvothermal, microwave-assisted solvothermal and conventional methods, respectively. The data were corrected taking into account the diamagnetic contribution of the sample holder and the samples. The single crystal X-ray diffraction data were obtained at room temperature with a Bruker Smart-CCD diffractometer using a Mo Kα (λ = 0.71073 Å) radiation. CCDC 1918138-1918140 contain the crystallographic data. These data can be obtained free of charge from the Cambridge Crystallographic Data Centre via www.ccdc.cam.ac.uk/data_request/cif. A summary of some crystal and refinement data can be found in Table 4. More information is shown in the Supplementary Material.

Table 4. Crystal and refinement data for **1–3**.

	1	**2**	**3**
Formula	$C_{40}H_{48}BF_4N_4O_6Ru_2$	$C_{33}H_{32}N_5O_4Ru_2S$	$C_{33}H_{32}N_5O_4Ru_2S$
fw	969.77	796.83	796.83
Space group	$P\bar{1}$	$P\bar{1}$	$P\bar{1}$
a/Å	10.4084(8)	11.4616(15)	11.158(3)
b/Å	10.90758(3)	11.6233(15)	12.746(3)
c/Å	11.2986(9)	14.6351(19)	14.768(3)
α/°	67.0540(10)	99.536(2)	66.649(4)
β/°	67.4970(10)	106.323(2)	75.001(4)
γ/°	71.4570(10)	106.346(2)	69.244(4)
V/Å^3	1069.59(14)	1730.9(4)	1785.9(7)
Z	1	2	2
d calc/*g*·cm^{-3}	1.506	1.529	1.482
μ/mm^{-1}	0.772	0.975	0.945
R indices	R_1 = 0.0627	R_1 = 0.0671	R_1 = 0.0735
(I ≥ 2σ (I))	wR_2 = 0.1934	wR_2 = 0.1607	wR_2 = 0.2081
GooF on F^2	1.092	1.027	1.010

3.2. Synthesis

3.2.1. Synthesis of $[Ru_2(\mu\text{-}NHOCC_6H_4\text{-}o\text{-}Me)_4(THF)_2](BF_4)$ (1)

0.15 mmol of $[Ru_2Cl(\mu\text{-}NHOCC_6H_4\text{-}o\text{-}Me)_4]_n$ (0.120 g) were suspended in 40 mL of THF and 0.15 mmol (0.030 g) of $AgBF_4$ were added to the solution. The mixture was stirred for 24 h at room temperature protected from light with aluminium foil. A white precipitate of AgCl and a brown

solution were obtained. The mixture was filtered using Celite and the solvent was evaporated under vacuum, producing a brown oily product. FT-IR (cm^{-1}): 3620w, 3334w, 3063w, 2959w, 2876w, 1605w, 1578w, 1563w, 1511m, 1460s, 1431s, 1293w, 1257w, 1230m, 1201w, 1139m, 1098s, 1037s, 918w, 868m, 852m, 784s, 732s, 667s. Single crystals of **1** were obtained by the following procedure: The brown product obtained as described above was dissolved in 8 mL of THF and mixed with two drops of toluene in a Teflon-lined solvothermal reactor. The mixture was heated in an oven for 24 h at 80 °C and slowly cool down to room temperature in 24 h.

3.2.2. Synthesis of $[Ru_2(SCN)(\mu\text{-}NHOCR)_4]_n$ (R = o-Me-C_6H_4 (2), m-Me-C_6H_4 (3), p-Me-C_6H_4 (4))

0.15. mmol (0.030 g) of $AgBF_4$ were added to a suspension of 0.15 mmol (0.120 g) of the corresponding $[Ru_2Cl(\mu\text{-}NHOCR)_4]_n$ (R = *o-Me*-C_6H_4, *m-Me*-C_6H_4, *p-Me*-C_6H_4) compound in 40 mL of THF. The mixture was protected from light with aluminium foil and was stirred for 24 h at room temperature, producing a white precipitate of AgCl and a brown solution. The AgCl was removed through filtration using Celite. The solvent was removed in vacuo obtaining a brown oily solid of the corresponding $[Ru_2(\mu\text{-}NHOCC_6H_4R)_4(THF)_2](BF_4)$ which was not isolated. This product was dissolved in 10 mL of methanol and 3.00 mmol of $(NBu_4)(SCN)$ (0.90 g) were added to the solution. Then, the reaction mixture was treated following one of the following procedures:

(a) The mixture was stirred at room temperature for 48 h obtaining a brown solid. The solid was filtered and washed with cold methanol (2 × 10 mL), diethyl ether (5 mL) and hexane (5 mL). (**2**): Yield: 0.03 g (24%). Anal. Calcd. (%) for **2**·3H_2O: C, 46.58; H, 4.50; N, 8.23; S, 3.77. Found (%): C, 46.44; H, 3.78; N, 8.19; S, 3.78. FT-IR (cm^{-1}): 3372w, 3322w, 3058w, 2967w, 2923w, 2077s, 1980w, 1937w, 1603w, 1578w, 1509s, 1479sh, 1458s, 1381m, 1283w, 1217m, 1198m, 1160w, 1139s, 1100s, 1043m, 946w, 903w, 851m, 782s, 729s, 665s. (**3**): Yield: 0.053 g (44%). Anal. Calcd. (%) for **3**·2H_2O: C, 47.59; H, 4.36; N, 8.41; S, 3.85. Found (%): C, 47.68; H, 3.94; N, 8.39. S, 3.73. FT-IR (cm^{-1}): 3336w, 3018w, 2920w, 2104w, 1957s, 1942s, 1591w, 1507s, 1460s, 1432s, 1321w, 1285w, 1249m, 1207m, 1190m, 1115s, 1085m, 1039w, 918w, 879w, 784s, 728s, 690m, 677m, 661w. ESI^+, *m*/*z* = 740.0, $[Ru_2(NHOCC_6H_4\text{-}m\text{-}Me)_4]^+$. (**4**): Yield: 0.079 g (66%). Anal. Calcd. (%) for **4**·2H_2O: C, 47.59; H, 4.36; N, 8.41; S, 3.85. Found (%): C, 48.04; H, 4.29; N, 8.16. S, 3.80. FT-IR (cm^{-1}): 3362w, 3022w, 2918w, 2088m, 1956w, 1611w, 1524m, 1488m, 1442s, 1289w, 1227w, 1208w, 1186m, 1122w, 1019w, 849w, 831w, 780w, 738s, 666w. ESI^+, *m*/*z* = 740.1, $[Ru_2(NHOCC_6H_4\text{-}p\text{-}Me)_4]^+$.

(b) The mixture was transferred into a Teflon-lined solvothermal reactor that was heated under the following program in a programmable oven: (i) 2 h heating ramp to reach 80 °C, (ii) 24 h isotherm at 80 °C, (iii) 16 h cooling ramp to room temperature. The brown solid obtained was filtered and washed with the same solvents used in procedure (a). (**2**): Yield: 0.026 g (22%). Anal. Calcd. (%) for **2**·H_2O: C, 48.64; H, 4.21; N, 8.59; S, 3.93. Found (%): C, 48.23; H, 3.92; N, 8.60; S, 3.95. FT-IR (cm^{-1}): 3372w, 3322w, 3058w, 2967w, 2923w, 2077s, 1980w, 1937w, 1603w, 1578w, 1509s, 1479sh, 1458s, 1381m, 1283w, 1217m, 1198m, 1160w, 1139s, 1100s, 1043m, 946w, 903w, 851m, 782s, 729s, 665s. UV-Vis-NIR: [λ, nm] 269, 352, 466, 598sh, 967. ESI^+, *m*/*z* = 740.0, $[Ru_2(NHOCC_6H_4\text{-}o\text{-}Me)_4]^+$. (**3**): Yield: 0.064 g (54%). Anal. Calcd. (%) for **3**·H_2O: C, 48.64; H, 4.21; N, 8.59; S, 3.93. Found (%): C, 48.74; H, 4.02; N, 8.48; S, 4.08. FT-IR (cm^{-1}): 3336w, 3018w, 2920w, 2104w, 1957s, 1942s, 1591w, 1507s, 1460s, 1432s, 1322w, 1285w, 1249m, 1208m, 1190m, 1115m, 1039w, 1005w, 879w, 784s, 728s, 689m, 677m, 660w. UV-Vis-NIR: [λ, nm] 314, 360sh, 476, 592sh, 1000. ESI^+, *m*/*z* = 740.1, $[Ru_2(NHOCC_6H_4\text{-}m\text{-}Me)_4]^+$. (**4**): Yield: 0.075 g (63%). Anal. Calcd. (%) for **4**·3H_2O: C, 46.58; H, 4.50; N, 8.23; S, 3.77. Found (%): C, 46.56; H, 4.14; N, 8.00. S, 4.00. FT-IR (cm^{-1}): 3362w, 3022w, 2918w, 2088m, 1956w, 1611m, 1524m, 1488m, 1442s, 1289w, 1226m, 1207w, 1186m, 1120m, 1019w, 849w, 829m, 779m, 737s, 661w. UV-Vis-NIR: [λ, nm] 299, 362sh, 475, 592sh, 989. ESI^+, m/z = 740.1, $[Ru_2(NHOCC_6H_4\text{-}p\text{-}Me)_4]^+$.

(c) The mixture was transferred into a TFM Teflon-closed vessel for microwave assisted solvothermal reactions and heated with the following program: *i*) 20 min heating ramp to reach 80 °C, ii) 16 h isotherm at 80 °C, iii) 20 min cooling ramp to room temperature. The brown solid obtained was isolated as described in procedure (a). (**2**): Yield: 0.041 g (33%). Anal Calcd. (%) for **2**: C, 49.74; H, 4.05;

N, 8.79; S, 4.02. Found (%): C, 49.18; H, 4.06; N, 8.71; S, 4.07. FT-IR (cm^{-1}): 3372w, 3321w, 3058w, 2968w, 2925w, 2078s, 1981w, 1939w, 1603w, 1579w, 1512s, 1479sh, 1459s, 1381m, 1285w, 1216m, 1200m, 1159w, 1137s, 1100s, 1043m, 948w, 901w, 854m, 783s, 729s, 665s. ESI^+, m/z = 740.0, $[Ru_2(NHOCC_6H_4\text{-}o\text{-}Me)_4]^+$. (**3**): Yield: 0.040 g (33%). Anal. Calcd. (%) for **3**·H_2O: C, 48.64; H, 4.21; N, 8.59; S, 3.93. Found (%): C, 48.36; H, 3.97; N, 8.34; S, 3.79. FT-IR (cm^{-1}): 3336w, 3018w, 2920w, 2104w, 1957s, 1942s, 1591w, 1507s, 1460s, 1432s, 1322w, 1285w, 1249m, 1208m, 1190m, 1115m, 1085m, 1039w, 1005w, 879w, 784s, 728s, 689m, 677m, 660w. ESI^+, m/z = 740.1, $[Ru_2(NHOCC_6H_4\text{-m-}Me)_4]^+$. (**4**): Yield: 0.093 g (78%). Anal. Calcd. (%) for **4**·3H_2O: C, 46.58; H, 4.50; N, 8.23; S, 3.77. Found (%): C, 47.00; H, 4.12; N, 8.13. S, 3.83. FT-IR (cm^{-1}): 3362w, 3022w, 2918w, 2088m, 1956w, 1611w, 1524m, 1488m, 1442s, 1289w, 1226w, 1207w, 1186m, 1121m, 1019w, 849w, 828m, 779m, 737s, 660w. ESI^+, m/z = 740.1, $[Ru_2(NHOCC_6H_4\text{-}p\text{-}Me)_4]^+$.

Crystals of **2** suitable for single crystal X-ray diffraction were obtained directly from the reaction described in the method b. Crystals of **3** suitable for single crystal X-ray diffraction were obtained by slow diffusion of a 10 mL methanol solution of 3 mmol $(NBu_4)(SCN)$ (0.90 g) into a 90 mL THF solution of $[Ru_2(\mu\text{-}NHOCC_6H_4\text{-}m\text{-}Me)_4(THF)_2](BF_4)$ obtained by reaction of 0.15 mmol of $[Ru_2Cl(\mu\text{-}NHOCC_6H_4\text{-}m\text{-}Me)_4]_n$ (0.120 g) and 0.15 mmol (0.030 g) of $AgBF_4$.

4. Conclusions

One dimensional zigzag coordination polymers of the type $[\{Ru_2(\mu\text{-}NHOCR)_4\}(\mu\text{-}SCN)]_n$ (R = *o*-Me-C_6H_4 (**2**), *m*-Me-C_6H_4 (**3**), *p*-Me-C_6H_4 (**4**)) can be prepared by reaction of the corresponding $[Ru_2(\mu\text{-}NHOR)_4(THF)_2](BF_4)$ compound with $(NBu_4)(SCN)$ at room temperature and also under solvothermal and microwave-assisted solvothermal methods. Differences in the steric hindrance of the *ortho*, *meta* and *para* configurations are probably responsible of the fact that **4** was obtained with higher yields than **3** and that the lowest yields were obtained in the synthesis of **2**. The resolution of the crystal structure of **2** and **3** showed that these polymers display a zigzag chain structure and also that linkage isomerism of the SCN^- ligands is observed in neighbouring valent-averaged dimetallic units. The magnetic data collected for compounds **2**–**4** are consistent with the existence of a S = 3/2 ground state, a large zero-field splitting and small antiferromagnetic interactions between dimetallic units.

Supplementary Materials: The following are available online at http://www.mdpi.com/2312-7481/5/3/40/s1, Crystal data and structure refinement, bond lengths and bond angles for **1**–**3**. Asymmetric units of **1**–**3**. Representation of the π-π stacking observed in the structure of **1**. Magnetic molar susceptibility and magnetic moment versus temperature for compounds **2** and **3**.

Author Contributions: R.J.-A. and J.-L.P. conceived and designed the experiments; S.M.-D.S., P.D.-M. and M.C. performed the experiments; P.D.-M. solved the crystal structures; R.G.-P., S.H. and R.J.-A. analysed the magnetic data; M.C., R.G.-P. and R.J.-A. wrote the manuscript.

Funding: This research was funded by the Spanish Ministerio de Economía y Competitividad (project CTQ2015-63858-P, MINECO/FEDER) and Comunidad de Madrid (project B2017/BMD-3770-CM).

Conflicts of Interest: The authors declare no conflict of interest.

References

1. Cotton, F.A.; Walton, R.A. *Multiple Bonds between Metal Atoms*, 2nd ed.; Wiley: New York, NY, USA, 1982.
2. Cotton, F.A.; Murillo, C.A.; Walton, R.A. *Multiple Bonds between Metal Atoms*, 3rd ed.; Springer: New York, NY, USA, 2005.
3. Aquino, M.A.S. Diruthenium and diosmium tetracarboxylates: Synthesis, physical properties and applications. *Coord. Chem. Rev.* **1998**, *170*, 141–202. [CrossRef]
4. Aquino, M.A.S. Recent developments in the synthesis and properties of diruthenium tetracarboxylates. *Coord. Chem. Rev.* **2004**, *248*, 1025–1045. [CrossRef]
5. Liddle, S.T. (Ed.) *Molecular Metal-Metal Bonds: Compounds, Synthesis, Properties*; Wiley-VCH: Weinheim, Germany, 2015.
6. Malinski, T.; Chang, D.; Feldmann, F.N.; Bear, J.L.; Kadish, K.M. Electrochemical Studies of a Novel Ruthenium(II, III) Dimer, $Ru_2(HNOCCF_3)_4Cl$. *Inorg. Chem.* **1983**, *22*, 3225–3233. [CrossRef]

7. Chavan, M.Y.; Feldmann, F.N.; Lin, X.Q.; Bear, J.L.; Kadish, K.M. Electrochemical Generation of New Dinuclear Ruthenium Acetamidate Complexes. *Inorg. Chem.* **1984**, *23*, 2373–2375. [CrossRef]
8. Barral, M.C.; Jiménez-Aparicio, R.; Monge, A.; Priego, J.L.; Royer, E.C.; Ruíz-Valero, C.; Urbanos, F.A. Tert-Butylbenzamidate diruthenium(II, III) Compounds. Crystal Structure of $[Ru_2(\mu\text{-}HNOC_6H_4\text{-}p\text{-}CMe_3)_4(OPPh_3)_2][BF_4]$. *Polyhedron* **1993**, *12*, 2947–2953. [CrossRef]
9. Chakravarty, A.R.; Cotton, F.A.; Tocher, D.A. Synthesis and Structure of a Binuclear Ruthenium 4-Chloro-Benzamidato Complex. *Polyhedron* **1985**, *4*, 1097–1102. [CrossRef]
10. Chakravarty, A.R.; Cotton, F.A. Structure of a Diruthenium(II, III) Complex with Benzamidato Bridging Ligands. *Polyhedron* **1985**, *4*, 1957–1958. [CrossRef]
11. Ryde, K.; Tocher, D.A. The Electro-oxidation of the Binuclear Ruthenium(II/III) Tetra-amidate Complex, $Ru_2(Me_3CCONH)_4Cl$. *Inorg. Chim. Acta* **1986**, *118*, L49–L51. [CrossRef]
12. Delgado, P.; González-Prieto, R.; Jiménez-Aparicio, R.; Perles, J.; Priego, J.L.; Torres, M.R. Comparative study of different methods for the preparation of tetraamidato and tetracarboxylatodiruthenium compounds. Structural and magnetic characterization. *Dalton Trans.* **2012**, *41*, 11866–11874. [CrossRef]
13. Delgado-Martínez, P.; González-Prieto, R.; Gómez-García, C.J.; Jiménez-Aparicio, R.; Priego, J.L.; Torres, M.R. Structural, magnetic and electrical properties of one-dimensional tetraamidatodiruthenium compounds. *Dalton Trans.* **2014**, *43*, 3227–3237. [CrossRef]
14. Delgado-Martínez, P.; Freire, C.; González-Prieto, R.; Jiménez-Aparicio, R.; Priego, J.L.; Torres, M.R. Synthesis, Crystal Structure, and Magnetic Properties of Amidate and Carboxylate Dimers of Ruthenium. *Crystals* **2017**, *7*, 192. [CrossRef]
15. Villalobos, L.; Cao, Z.; Fanwick, P.E.; Ren, T. Diruthenium(II, III) tetramidates as a new class of oxygenation catalysts. *Dalton Trans.* **2012**, *41*, 644–650. [CrossRef] [PubMed]
16. Ebihara, M.; Fuma, Y. Two- and three-dimensional assembled structures constructed from amidate-bridged paddlewheel complexes with group 6 oxometallate ions. *Acta Cryst.* **2013**, *B69*, 480–489. [CrossRef] [PubMed]
17. Burmeister, J. Ambidentate ligands, the schizophrenics of coordination chemistry. *Coord. Chem. Rev.* **1990**, *105*, 77–133. [CrossRef]
18. Brewster, T.P.; Ding, W.; Schley, N.D.; Hazari, N.; Batista, V.S.; Crabtree, R.H. Thiocyanate Linkage Isomerism in a Ruthenium Polypyridyl Complex. *Inorg. Chem.* **2011**, *50*, 11938–11946. [CrossRef]
19. Mautner, F.A.; Albering, J.H.; Harrelson, E.V.; Gallo, A.A.; Massoud, S.S. N-bonding vs. S-bonding in thiocyanato-copper(II) complexes. *J. Mol. Struct.* **2011**, *1006*, 570–575. [CrossRef]
20. Mautner, F.A.; Fischer, R.C.; Rashmawi, L.G.; Louka, F.R.; Massoud, S.S. Structural characterization of metal(II) thiocyanato complexes derived from bis(2-(H-pyrazol-1-yl)ethyl)amine. *Polyhedron* **2017**, *124*, 237–242. [CrossRef]
21. Mekuimemba, C.D.; Conan, F.; Mota, A.J.; Palacios, M.A.; Colacio, E.; Triki, S. On the Magnetic Coupling and Spin Crossover Behavior in Complexes Containing the Head-to-Tail $[Fe_2^{II}(\mu\text{-}SCN)_2]$ Bridging Unit: A Magnetostructural Experimental and Theoretical Study. *Inorg. Chem.* **2018**, *57*, 2184–2192. [CrossRef]
22. Rams, M.; Tomkowicz, Z.; Böhme, M.; Plass, W.; Suckert, S.; Werner, J.; Jessc, I.; Näther, C. Influence of metal coordination and co-ligands on the magnetic properties of 1D $Co(NCS)_2$ coordination polymers. *Phys. Chem. Chem. Phys.* **2017**, *19*, 3232–3243. [CrossRef]
23. Shurdha, E.; Moore, C.E.; Rheingold, A.L.; Lapidus, S.H.; Stephens, P.W.; Arif, A.M.; Miller, J.S. First Row Transition Metal(II) Thiocyanate Complexes, and Formation of 1-, 2-, and 3-Dimensional Extended Network Structures of $M(NCS)_2(Solvent)_2$ (M = Cr, Mn, Co) Composition. *Inorg. Chem.* **2013**, *52*, 10583–10594. [CrossRef]
24. Nebbali, K.; Mekuimemba, C.D.; Charles, C.; Yefsah, S.; Chastanet, G.; Mota, A.J.; Colacio, E.; Triki, S. One-Dimensional Thiocyanato-Bridged Fe(II) Spin Crossover Cooperative Polymer With Unusual FeN_5S Coordination Sphere. *Inorg. Chem* **2018**, *57*, 12338–12346. [CrossRef] [PubMed]
25. Wang, D.; Yang, H.-Q.; Wu, G.-H.; Hou, X.-F.; Yang, J.-H.; Liu, B. Mixed-valent diruthenium diphosphonate containing zigzag chain structure of $\{Ru_2(hedp)_2(SCN)\}_n^{4n-}$. *Inorg. Chem. Commun.* **2014**, *46*, 241–243. [CrossRef]
26. Barral, M.C.; González-Prieto, R.; Herrero, S.; Jiménez-Aparicio, R.; Priego, J.L.; Royer, E.C.; Torres, M.R.; Urbanos, F.A. Synthesis and crystal structure of high and low spin diruthenium complexes with diphenylformamidine and diphenyltriazene ligands. *Polyhedron* **2004**, *23*, 2637–2644. [CrossRef]

27. Nguyen, M.; Phan, T.; Van Caemelbecke, E.; Wei, X.; Bear, J.L.; Kadish, K.M. Synthesis and Characterization of (3,1) $Ru_2(F_3ap)_4(NCS)$ and (3,1) $Ru_2(F_3ap)_3(F_2Oap)(NCS)$ Where F_3ap Is the 2-(2,4,6-Trifluoroanilino) pyridinate Anion. *Inorg. Chem.* **2008**, *47*, 4392–4400. [CrossRef] [PubMed]
28. Miskowski, V.M.; Loehr, T.M.; Gray, H.B. Electronic and vibrational spectra of $Ru_2(carboxylate)_4^+$ complexes. Characterization of a high-spin metal-metal ground state. *Inorg. Chem.* **1987**, *26*, 1098–1108. [CrossRef]
29. Miskowski, V.M.; Gray, H.B. Electronic spectra of $Ru_2(carboxylate)_4^+$ complexes. Higher energy electronic excited states. *Inorg. Chem.* **1988**, *27*, 2501–2506. [CrossRef]
30. Miskowski, V.M.; Hopkins, M.D.; Winkler, J.R.; Gray, H.B. *Inorganic Structure and Spectroscopy*; John Wiley and Sons: New York, NY, USA, 1999.
31. Castro, M.A.; Roitberg, A.E.; Cukiernik, F.D. Theoretical and Experimental Studies of Diruthenium Tetracarboxylates Structure, Spectroscopy, and Electrochemistry. *Inorg. Chem.* **2008**, *47*, 4682–4690. [CrossRef]
32. Barral, M.C.; González-Prieto, R.; Jiménez-Aparicio, R.; Priego, J.L.; Torres, M.R.; Urbanos, F.A. Synthesis, Properties, and Structural Characterization of Bromo- and Iodotetracarboxylatodiruthenium(II,III) Compounds. *Eur. J. Inorg. Chem.* **2004**, *2004*, 4491–4501. [CrossRef]
33. Clark, R.J.H.; Franks, M.L. Resonance Raman spectra of chlorotetra-acetato- and chlorotetrabutyrato-diruthenium. *J. Chem. Soc. Dalton Trans.* **1976**, 1825–1828. [CrossRef]
34. Clark, R.J.H.; Ferris, L.T.H. Resonance Raman, excitation profile and electronic structural studies of diruthenium tetracarboxylate complexes. *Inorg. Chem.* **1981**, *20*, 2759–2766. [CrossRef]
35. Barral, M.C.; de la Fuente, I.; Jiménez-Aparicio, R.; Priego, J.L.; Torres, M.R.; Urbanos, F.A. Synthesis of diruthenium(II,III) amidate compounds. Crystal structure of $[Ru_2(\mu\text{-}HNOCC_4H_3S)_4(thf)_2]SbF_6 \cdot 0.5$cyclohexane. *Polyhedron* **2001**, *20*, 2537–2544. [CrossRef]
36. Handa, M.; Yano, N.; Okuno, A.; Nakai, H.; Mitsumi, M.; Mikuriya, M.; Kataoka, Y. Synthesis, Structure and Magnetic and Electrochemical Properties of Tetrakis(benzamidato)diruthenium(II,III) Tetrafluoroborate. *Magnetochemistry* **2018**, *4*, 21. [CrossRef]
37. Ebihara, M.; Fuma, Y. Tetra-μ-acetamidato- κ^4N:Oκ^4O:N-bis[aquaruthenium(II,III)](Ru-Ru) perchlorate. *Acta Cryst. Sect. E* **2006**, *62*, m2802–m2804.
38. Ebihara, M.; Fuma, Y. Tetra-μ-acetamidato- κ^4N:Oκ^4O:N-bis[aquaruthenium(II,III)](Ru-Ru) nitrate. *Acta Cryst. Sect. E* **2006**, *62*, m2805–m2807.
39. Ebihara, M.; Fuma, Y. Tetra-μ-acetamidato- κ^4N:Oκ^4O:N-bis[aquaruthenium(II,III)](Ru-Ru) tetraphenylborate monohydrate. *Acta Cryst. Sect. E* **2006**, *62*, m2808–m2810.
40. Zhang, H.-X.; Ke, W.-S.; Zhu, C.-Y.; Wang, J.-Y.; Sasaki, Y.; Chen, Z.-N.; Lin, C.; Wang, Z.; Liao, S.; Wu, W. Synthesis, characterization and properties of oxo-bridged diruthenium(III) complexes with thiocyanato and cyanato ligands. *Inorg. Chim. Acta* **2018**, *469*, 469–477. [CrossRef]
41. Norman, G.J.; Renzoni, G.E.; Case, D.A. Electronic Structure of $Ru_2(O_2CR)_4^+$ and $Rh_2(O_2CR)_4^+$ Complexes. *J. Am. Chem. Soc.* **1979**, *101*, 5256–5267. [CrossRef]
42. Barral, M.C.; Jiménez-Aparicio, R.; Pérez-Quintanilla, D.; Priego, J.L.; Royer, E.C.; Torres, M.R.; Urbanos, F.A. Magnetic Properties of Diruthenium(II,III) Carboxylate Compounds. Crystal Structures of $Ru_2Cl(\mu\text{-}O_2CCHCHCHCHMe)_4$ and $Ru_2Cl(\mu\text{-}O_2CCH_2OMe)_4$. *Inorg. Chem.* **2000**, *39*, 65–70. [CrossRef]
43. Mikuriya, M.; Yoshioka, D.; Handa, M. Magnetic interactions in one-, two-, and three-dimensional assemblies of dinuclear ruthenium carboxylates. *Coord. Chem. Rev.* **2006**, *250*, 2194–2211. [CrossRef]
44. Cukiernik, F.D.; Luneau, D.; Marchon, J.-C.; Maldivi, P. Mixed-Valent Diruthenium Long-Chain Carboxylates. 2. Magnetic Properties. *Inorg. Chem.* **1998**, *37*, 3698–3704. [CrossRef]
45. Khan, O. *Molecular Magnetism*; VCH Publisher Inc.: New York, NY, USA, 1993.